Agr. Nat. Resour. 57 (2023) 163–172

AGRICULTURE AND NATURAL RESOURCES

Journal homepage: http://anres.kasetsart.org

Research article

Effectiveness of adsorption of alizarin red s and alizarin yellow 2G from aqueous solutions using zeolite L

Wilaiporn Insuwan[a,*], Saowaluck Srihongthong[a], Navaphum Permngam[a], Pongsathorn Tongkasee[b]

[a] *Department of Science and Mathematics, Faculty of Agriculture and Technology, Rajamangala University of Technology Isan Surin Campus, Surin 32000, Thailand*

[b] *Department of Thai Traditional Medicine, Faculty of Natural Resources, Rajamangala University of Technology Isan Sakon Nakhon Campus, Sakon Nakhon 76000, Thailand*

Article Info

Article history:
Received 8 August 2022
Revised 8 December 2022
Accepted 22 December 2022
Available online 28 February 2023

Keywords:
Adsorption isotherm,
Anionic dye,
Kinetics,
Removal,
Zeolite L

Abstract

Importance of the work: Zeolite L in potassium form (KLTL) was used as an alternative adsorbent for the adsorption of alizarin red s (ARS) and alizarin yellow 2G (ARY) from aqueous solutions.

Objectives: To use KLTL as an alternative adsorbent for the removal of two anionic dyes from aqueous solutions.

Materials & Methods: The adsorption performance was determined by adsorption equilibrium, kinetics, and thermodynamic parameters.

Results: The optimum adsorbent dosage and contact time were 0.025 g and 120 min, respectively. The adsorption isotherm and kinetics followed the Langmuir isotherm, the maximum monolayer adsorption capacity was 95.24 mg/g and 41.30 mg/g for ARS and ARY, respectively, while the mechanism of adsorption followed a nonlinear pseudo-first-order model. All anionic dyes were adsorbed onto KLTL via an electrostatic interaction and H-bond. In addition, thermodynamic parameters such as $\Delta G°$, and $\Delta H°$ were investigated and suggested that the adsorption of the anionic dyes onto KLTL was the spontaneous and endothermic reaction.

Main finding: This was the first study on the adsorptive removal of the anionic ARS and ARY dyes using KLTL as an adsorbent. The results of the study are important for industrial applications.

* Corresponding author.
E-mail address: wi_insuwan@hotmail.com (W. Insuwan)

https://doi.org/10.34044/j.anres.2023.57.1.17

Introduction

Dyes are extensively used in a wide range of industries, such as food, textile, pharmaceutical and cosmetic production. However, toxins from the textile, plastic and cosmetic industries contribute many contaminants that pollute streams (Tsuboy et al., 2007; Li et al., 2011; Venkatesh, 2019). Alizarin red s (ARS) and alizarin yellow 2G (ARY) are two carcinogenic anionic dyes widely used in cotton textiles, paper and cosmetics and they are often used as a stain to identify calcium-containing osteocytes in differentiated cultures of human and rodent mesenchymal stem cells, whose structure is shown in Fig. 1 (Paul et al., 1983). As a result, dyes must be removed from wastewater to preserve environment and human health. Many methods have been developed to treat polluted wastewater, such as coagulation sedimentation, filtration, photocatalytic degradation and adsorption (Bhomick et al., 2020).

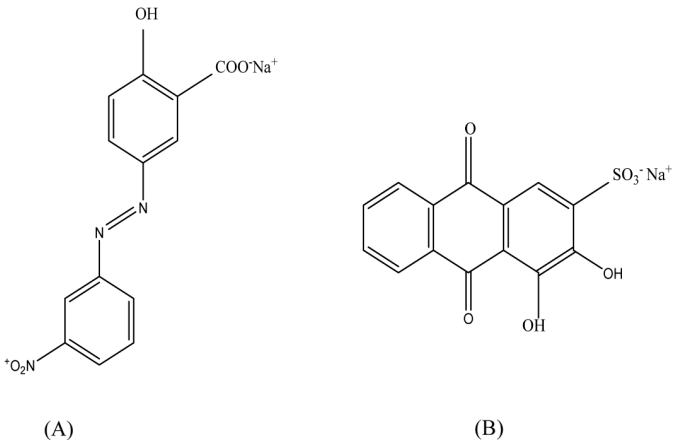

(A) (B)

Fig. 1 Chemical structures of: (A) alizarin yellow 2G; (B) alizarin red s

Adsorption has become one of the most popular wastewater treatment technologies due to its high efficiency, cleanliness and simplicity (Slimani et al., 2021). According to the literature review, maghemite nano adsorbent, immobilized root tuber of *Canna indica* beads (Venkatesh, 2019), carbon nanotube (Zhang et al., 2019), multi-walled carbon nanotubes (Ghaedi et al., 2011) and activated clay (Fu et al., 2011) have all been described as adsorbents. The current study investigated the removal of dyes using zeolite L (KLTL) as an adsorbent. It is widely used in the removal of dyes due to its high thermal stability, good textural properties and strong adsorption ability (Insuwan, 2013; Insuwan and Rangsriwatananon, 2014). These authors have reported that KLTL frameworks are generally anionic to maintain electrical neutrality, while charge-balancing cations (K^+) populate the pores; in ion exchange, these cations can interact with organic cations, water and dye molecules. The current study removed dyes from aqueous solutions using KLTL as an adsorbent. The effects of various influencing factors (adsorbent dosage, contact time and temperature) were thoroughly examined. In addition, the kinetics and thermodynamics of alizarin red s (ARS) and alizarin yellow 2G (ARY) adsorption were analyzed and discussed.

Materials and Methods

Adsorbent: The typical procedure for the preparation of KLTL synthesis was adapted from Insuwan and Rangsriwatananon (2012). Aluminum hydroxide was dissolved in potassium hydroxide solution (solution A). The silica solution was prepared by adding LUDOX HS 40 to distilled water (solution B). Next, solution A was slowly added to solution B. The mixture was stirred for 5 min to obtain a homogeneous mixture gel. After that, the gel was transferred into a Teflon-lined autoclave at 453 K for 2 d. Then, the autoclave was cooled in cold water before opening. The final product was washed with distilled water until the pH of the liquid was neutral, after which the crystal was dried for 12 h at 353 K in a hot air oven.

Adsorbate: Alizarin red s (ARS) and alizarin yellow 2G (ARY) were obtained from Sigma Aldrich. A 1,000 parts per million (ppm; in milligrams per liter) stock solution was obtained performed by dissolving 1.0 g of the dyes in 1 L of deionized water.

Adsorbent characterization

Scanning electron microscopy (SEM; JSM6400; JEOL) with an acceleration voltage of 5 kV was used to confirm the morphology of KLTL.

Adsorption studies

Adsorption was carried out to investigate the adsorbent dosage, isotherm adsorption and kinetics. The investigation was carried out in 125 mL Erlenmeyer flask with 25 mL of dye solution, 30 ppm, achieved by diluting the dye stock solution and adding a small amount of adsorbent (0.010–0.150 g). The mixture was agitated in a shaker bath at 303 K for 12 h. The adsorbent was removed using centrifugation at 5,000 revolutions per minute for 5 min. An ultraviolet-visible spectrophotometer was used to measure the concentration of the residual dyes in solution before and after adsorption whose wavelengths were fixed at 420 nm and 340 nm for ARS and ARY, respectively, as shown in Fig. 2.

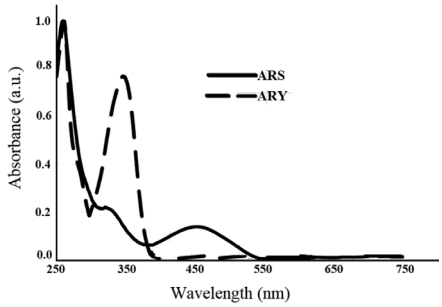

Fig. 2 Normalized absorption spectra of alizarin red s (ARS) and alizarin yellow 2G (ARY) in aqueous solution

A kinetic study was performed on 0.025 g of KLTL combined with 100 mL of dye solution of 10, 3 0 or 50 ppm in an Erlenmeyer flask. Each mixture was shaken in a shaker bath at 303 K for 60 to 360 min (60, 120, 180, 240, 300 and 360 min). After that, the operation followed the same procedure as for the adsorbent dosage.

For the adsorption equilibrium study, 50 mL of dye solution was mixed with 0.025 g of KLTL. Each mixture was shaken in a shaker bath for 360 min at 303 K, 313 K or 323 K. Then, the operation followed the same procedure as for the adsorbent dosage. Finally, the amount of dye adsorbed onto the adsorbent (qe; in milligrams per gram) and the amount of dye adsorbed at any time (qt; in milligrams per gram) were calculated using Equations 1 and 2, respectively (Insuwan et al., 2020):

$$q_e = \frac{(C_0 - C_e)}{m} V \quad (1)$$

$$q_t = \frac{(C_0 - C_t)}{m} V \quad (2)$$

where C_0 and C_e (measured in milligrams per liter) are the initial concentration and the concentration of the adsorbate in solution, respectively, C_t (in milligrams per liter) is the concentration of the adsorbate in solution at any time, V (in liters) is the solution volume and m (in grams) is the mass of KLTL adsorbent.

Results and Discussion

Characterization of zeolite L

Fig. 3 shows the SEM images of KLTL. Part of the characterized pre-adsorption and post-adsorption using SEM was not examined. The studied sample had a round shape with dimensions of 1.375 µm × 1.295 µm. A previous study confirms that zeolite L (KLTL) with a round shape has a high adsorption capacity compared to zeolite L (KLTL) with an ice hockey shape. The results suggested that the round shape had more acid sites than the ice hockey shape (Insuwan and Rangsriwatananon, 2014). In addition, the adsorption capacities were related to the surface characteristics of the adsorbents that increased for a higher surface area. Insuwan and Saosai (2019) reported the surface area of KLTL as 348 m^2/g, which was higher than for activated carbon. Thus, the increased accessibility of active sites of zeolite LTL also improved the adsorption capacity.

Effect of adsorbent dosage

Fig. 4 shows the effects of adsorbent dosage in the range 0.010–0.150 g on dye adsorption. It was clear that the dye adsorption process occurred very quickly and reached a maximum adsorbent dosage of 0.025 g. After that, the absorption of both dyes reduced and was stable in the range 0.050–0.150 g. This could be explained by the increase in adsorbent dosage that also increased the number of adsorption sites. However, at an adsorbent dosage in the range 0.025–0.150 g, the amount of dye adsorbed onto the adsorbent decreased, indicating that the adsorbent was already saturated and could not incorporate any more dye at the adsorption site (Badran and Khalaf, 2020).

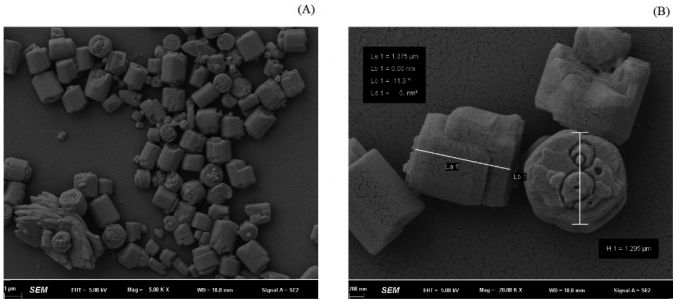

Fig. 3 Scanning electron microscopy images of Zeolite L at: (A) 5,000× magnification; (B) 20,000× magnification

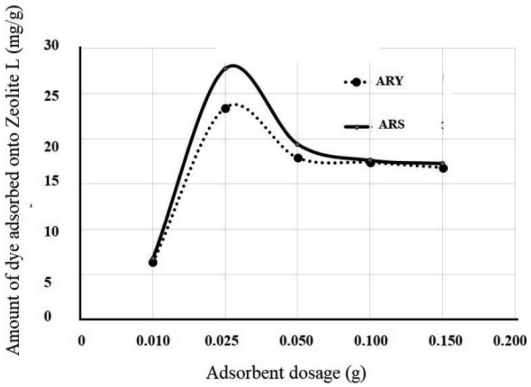

Fig. 4 The effect of adsorbent dosage on the amount of alizarin red s (ARS) and alizarin yellow 2G (ARY) dyes adsorbed onto zeolite L, where initial concentration was 30 parts per million and contact time was 12 h.

Effect of contact time

The optimal period for the adsorption procedure was investigated. The dye adsorbed onto KLTL had a contact time in the range 60–360 min. The initial research also examined the impact of dye concentrations (10–100 ppm) and indicated that the efficiency of the removal decreased as the concentration increased because at lower concentrations, the amount of dye was low compared to the available active sites of Zeolite L; however, when the concentration increased to 60 ppm, dye molecules were blocked on the surface of Zeolite L and could not be adsorbed. Therefore, 20–40 ppm was chosen as a suitable initial concentration. Fig. 5 shows the effect of contact time on the adsorption of ARS and ARY onto KLTL at different initial concentrations in the range 20–40 ppm. The results showed a similar trend for both dyes, with rapid adsorption for the first 60 min, slower adsorption for the next 120 min and then steady until 360 min. This implied that the dye uptake increased as time passed until it reached equilibrium at 120 min. After the dye molecules had occupied all the active sites of KLTL, the rate of adsorption was negligible. For the above reasons, it was determined that the appropriate time for dye adsorption was 120 min.

The adsorption isotherm is fundamental in the adsorption design process because it describes the interaction behavior between the adsorbate and the adsorbent. The Langmuir and Freundlich models, which are commonly used, have been found to describe the process accurately. The Langmuir and Freundlich equations can be written as Equations 3 and 4, respectively (Khayyun and Mseer, 2019):

$$q_{e=}\frac{q_m K_L C_e}{1+ K_L C_e} \quad (3)$$

$$q_{e=} K_F C_e{}^{1/n} \quad (4)$$

where q_e is the adsorbed value of dyes at equilibrium concentration (measured in milligrams per gram), q_m is the maximum adsorption capacity (in milligrams per gram), C_e is the equilibrium concentration of dyes in solution (in milligrams per liter), K_L is the Langmuir constant (in liters per milligram), K_F (mg/g·mg$^{-1/n}$·L$^{1/n}$) and 1/n are the Freundlich constants which indicate the adsorption capability and intensity, respectively.

The adsorption isotherms of ARS and alizarin yellow 2G onto KLTL are shown in Fig. 6. The results showed that both dyes consistently demonstrated an increase in adsorption with increasing temperature. This result suggested that an increased rate of dye molecule diffusion through the zeolite L pores may occur at higher temperatures. Additionally, when the

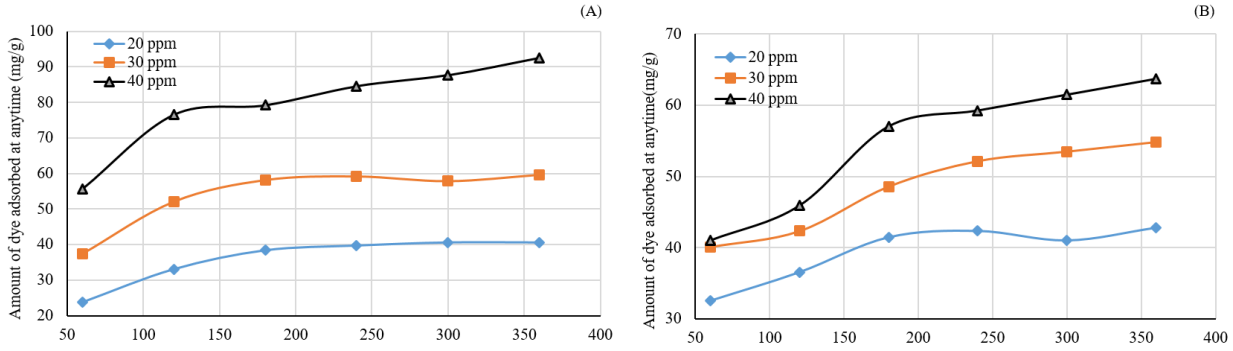

Fig. 5 Effect of contact time on adsorption of: (A) alizarin red s; and (B) alizarin yellow 2G, where ppm = parts per million

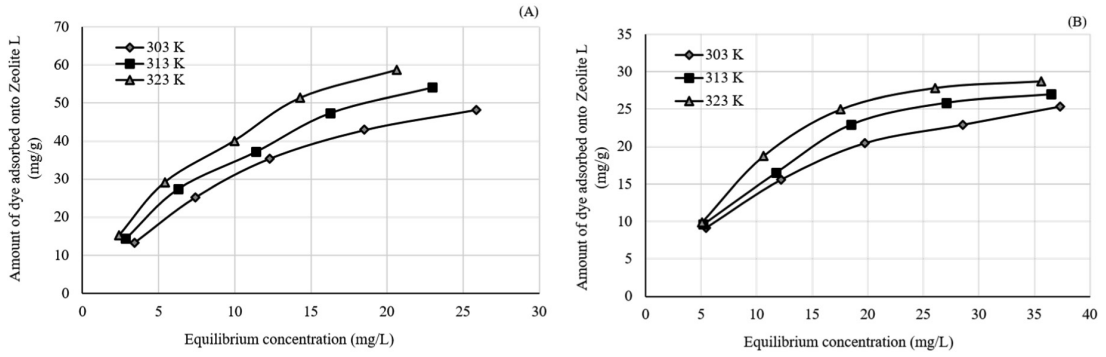

Fig. 6 adsorption isotherms of dyes adsorbed on zeolite L for adsorbed dosage = 0.025g and time = 120 min: (A) alizarin red s; (B) alizarin yellow 2G

temperature rises, the viscosity of the solution decreases and the mobility of the dye molecules that can move through the zeolite L pores also increases (Insuwan et al., 2020). Langmuir and Freundlich's models were fitted to the data for the adsorption of the dyes onto zeolite L. A linear plot of C_e/q_e versus C_e for ARS and ARY adsorbed onto zeolite L is illustrated in Fig. 7, and the Langmuir and Freundlich parameters are presented in Table 1.

The equilibrium data was a reasonably good fit to the Langmuir models and was better fitting than the Freundlich models based on the coefficient of determination (R^2) value that were greater than 0.9. The monolayer adsorption capacity (q_m) values of the ARS and ARY adsorbed on KLTL were 80.65–95.24 mg/g and 36.10–41.30 mg/g, respectively. In addition, the value of K_F was related to the degree of adsorption in that the ARS adsorbed on KLTL was higher than for ARY, indicating that ARS and KLTL had a stronger affinity than ARY (as shown in Fig. 8). ARS and ARY adsorbed onto KLTL can be described by two different types of interactions. The first is an electrostatic interaction, in which K^+ ions in the KLTL framework point toward the negatively charged sulfonate group (SO_3^-) and negatively charged carboxylic groups (COO^-) of the ARS and ARY, respectively. Secondly, H-bond interaction was shown to occur between the silica framework through the hydroxyl group of KLTL and the -OH groups of dye molecules (Bhomick et al., 2020). This corresponded with Jun et al. (2020) who demonstrated the applicability of the low-cost green adsorbents produced from zeolite-Fe/AC in the treatment

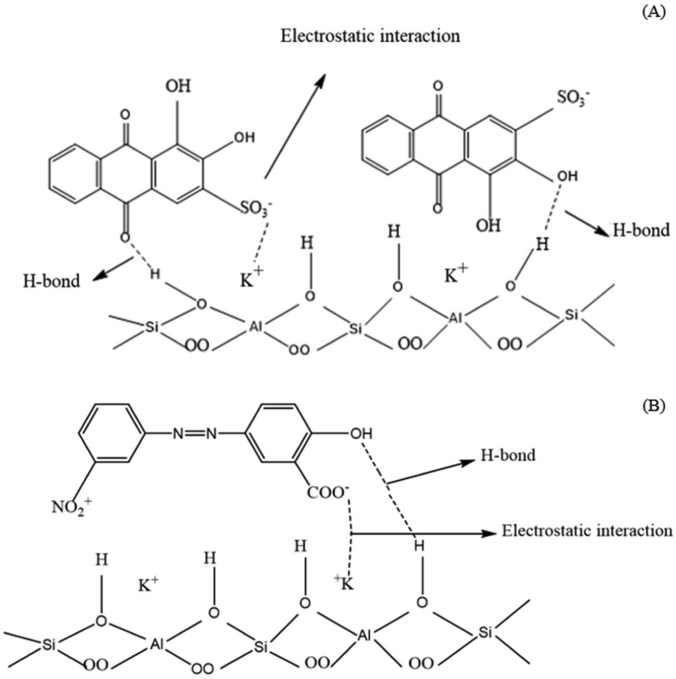

Fig. 8 Proposed adsorption mechanisms onto zeolite L of: ARS (A); and ARY (B)

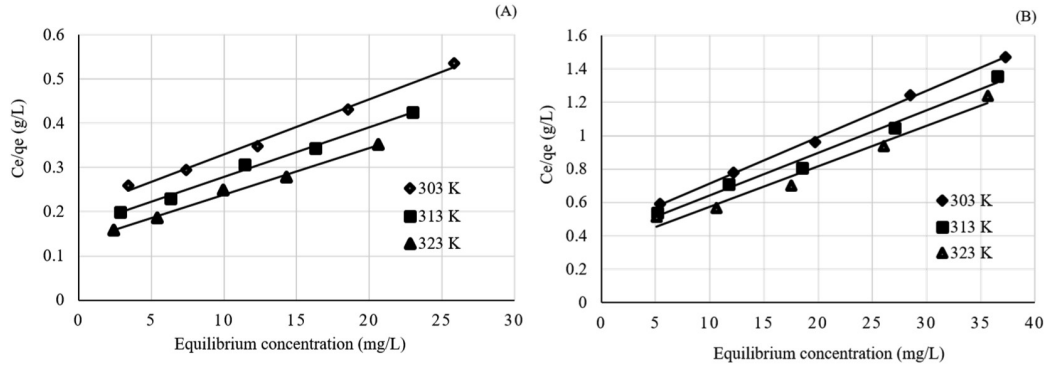

Fig. 7 Langmuir isotherm of dyes adsorbed on zeolite L (KLTL), adsorbed dosage = 0.025g and time = 120 min: (A) alizarin red s; (B) alizarin yellow 2G

Table 1 Langmuir and Freundlich parameters of alizarin red s and alizarin yellow 2G onto zeolite L

Dye molecule	Temp. (K)	Langmuir isotherm			Freundlich isotherm		
		K_L (L/mg)	q_m (mg/g)	R^2	K_F mg/g·g$^{-1/n}$·L$^{1/n}$	n	R^2
Alizarin red S	303	0.060	80.65	0.9931	5.050	1.544	0.9769
	313	0.067	89.29	0.9927	5.570	1.566	0.9862
	323	0.079	95.24	0.9929	6.040	1.580	0.9864
Alizarin yellow 2G	303	0.063	36.10	0.9985	3.7308	1.887	0.9804
	313	0.066	39.20	0.9851	3.8563	1.819	0.9625
	323	0.073	41.30	0.9723	4.0774	1.796	0.9251

q_m = maximum adsorption capacity, K_L = Langmuir constant, K_F and n are the Freundlich constants which indicate the adsorption capability and intensity, respectively and R^2 is coefficient of determination.

of oil refinery effluent based on the proposed adsorption mechanisms of the adsorption process with the aid of oxidants: 1) physical adsorption, 2) Fenton oxidation, 3) electrostatic interactions, 4) H-bonding interactions and 5) n–p interactions.

However, ARS had a greater adsorption capability at all temperatures than ARY. This may have been due to the nitro group ($-NO_2^+$) of ARY that caused enhanced repulsion with the cation (K^+) in the zeolite framework.

Thermodynamic parameters

Generally, the Van't Hoff equation, as shown in Equation 5 has been used to determine thermodynamic parameters, such as ($\Delta G°$, $\Delta H°$ and $\Delta S°$).

$$\ln K = \frac{-\Delta H^0}{RT} + \frac{\Delta S^0}{R} \quad (5)$$

where K is the equilibrium constant, R is the universal gas constant (8.314 J/mol/K) and T is the temperature (K). The plot of lnK versus 1/T gives a straight line with a slope and intercept (multiplied by R) representing $\Delta H°$ and $\Delta S°$, respectively. Gibbs free energy change ($\Delta G°$) is related to the spontaneity of adsorption, with the relationship between $\Delta G°$ and K shown by Equation 6:

$$\Delta G^0 = -RT\ln K \quad (6)$$

However, K in Equation (6) calculated using the Langmuir constant (K_L) cannot be substituted (Yoshida et al., 2020). The relationship between the equilibrium constant and the Langmuir constant can be written as Equation 7:

$$K = (K_L M_A/\gamma_e) \quad (7)$$

where M_A is the molecular weight of the adsorbent in milligrams per mol and γ_e is the activity coefficient that depends on the concentration of ionic adsorbate. In this situation, the activity coefficient provided by Equation 7 can be neglected for the diluted ionic solution and is given by Equation 8 (Yoshida et al., 2020):

$$K = K_L M_A \quad (8)$$

Table 2 shows the thermodynamic parameter values for ARS and ARY adsorption onto KLTL. The endothermic reaction and the physical adsorption of the two dyes were confirmed by the positive values of enthalpy change ($\Delta H°$ = 10.80 kJ/mol for ARS and 5.44 kJ/mol for ARY). $\Delta G°$ for adsorption was negative for all dyes, which indicated a spontaneous adsorption process. Additionally, an increase in randomness at the solid-solution interface was shown by the positive value of entropy change ($\Delta S°$).

The maximum monolayer adsorption capacity (q_m) values for ARS and ARY from the Langmuir equation were compared with the q_m values of other adsorbents in the literature as presented in Table 3.

Adsorption kinetics study

The mechanism of the adsorption of dyes onto zeolite L was investigated using pseudo-first-order and pseudo-second-order models, with the first model generally expressed as Equation 9 (Ho and McKay, 1998):

Table 2 Thermodynamic parameters for dye adsorption onto zeolite L

Dyes	Temperature (K)	$\Delta H°$ (kJ/mol)	$\Delta S°$ (kJ/mol/K)	$\Delta G°$ (kJ/mol)
Alizarin red s	303		0.1183	-25.03
	313	10.80	0.1180	-26.13
	323		0.1182	-27.39
Alizarin yellow 2G	303		0.0642	-24.90
	313	5.44	0.0651	-25.80
	323		0.0665	-26.90

Table 3 Comparison of maximum monolayer adsorption capacities of various adsorbents for alizarin red s (ARS) and alizarin yellow 2G (ARY)

Number	Adsorbent	Maximum monolayer adsorption capacity (q_m, mg/g)		Reference
		ARS	ARY	
1	Immobilized *Canna indica* beads	21.69	-	Venkatesh, 2019
2	Biomass-based activated carbon	91.695	-	Bhomick et al., 2020
3	Eggshells	156.56	-	Slimani et al., 2021
4	Activated clay modified by iron oxide	32.7	-	Fu et al., 2011
5	Polypyrrole-coated magnetic nanoparticle	116.3	113.6	Gholivand et al., 2015
6	Charcoal	-	14.93	Salman et al., 2011
7	Zeolite L	95.24	41.30	This work

$$q_t = q_e(1-e^{-k_1 t}) \quad (9)$$

This can be rearranged in a linearized form as Equation 10 (Biglari et al., 2018):

$$\ln(q_e - q_t) = \ln(q_e) - k_1 t \quad (10)$$

The first-order rate constant, k_1 (min^{-1}) is the linear plot of ln (q_e - q_t) versus t that gives the slope, with lnq_e as the intercept.

The pseudo-second-order kinetic model was initially proposed as a second-order rate equation for various studies (Ho and McKay, 1998; Moussout et al., 2018; Ngakou et al., 2019), based on the strong bond between the adsorbent and adsorbate, as shown in Equation 11:

$$q_t = \frac{q_e^2 k_2 t}{q_e k_2 t+1} \quad (11)$$

The pseudo-second-order model is used to predict the behavior of the adsorption process and the linear form is given as Equation 12 (Biglari et al., 2018):

$$\frac{t}{q_t} = \frac{1}{k_2 q_e^2} + \frac{1}{q_e} t \quad (12)$$

The second-order rate constant, k_2 (g/mg/min) and q_e were determined from the intercept and slope of the linear plot of ln t/q_t versus t, respectively.

In order to assess the best-fitting model for the experimental data, the standard deviation (Δq, as a percentage) and the coefficient of determination (R^2) are excellent statistical parameters for such a validation, which is shown in Equation 13 (Moussout et al., 2018):

$$\Delta q(\%) = \sqrt{\sum \frac{\left[\frac{q_{t.exp}-q_{t.cal}}{q_{t.exp}}\right]^2}{n-1}} x100 \quad (13)$$

where $q_{t.exp}$ and $q_{t.cal}$ are the experimental and calculated adsorption capacities, respectively, and n is the number of data points.

The results of fitting the experimental data to the pseudo-first-order and pseudo-second-order models are displayed in Figs. 9 and 10 and Table 4. The experimental data clearly agreed with the nonlinear pseudo-first order (NLPFO) model rather than the other models. However, the processing of the same experimental data using the linear pseudo-first-order (LPFO) and linear pseudo-second-order (LPSO) models led to a result that differed from the first, regardless of whether the value of R^2 was higher than 0.99. It was noted that determining R^2 alone is insufficient to choose between the kinetic models. Several reports recommended that nonlinear equations can be transformed into linear forms for isotherm models, which could lead to biases, such as low linearity, despite having strong linear regression coefficients,

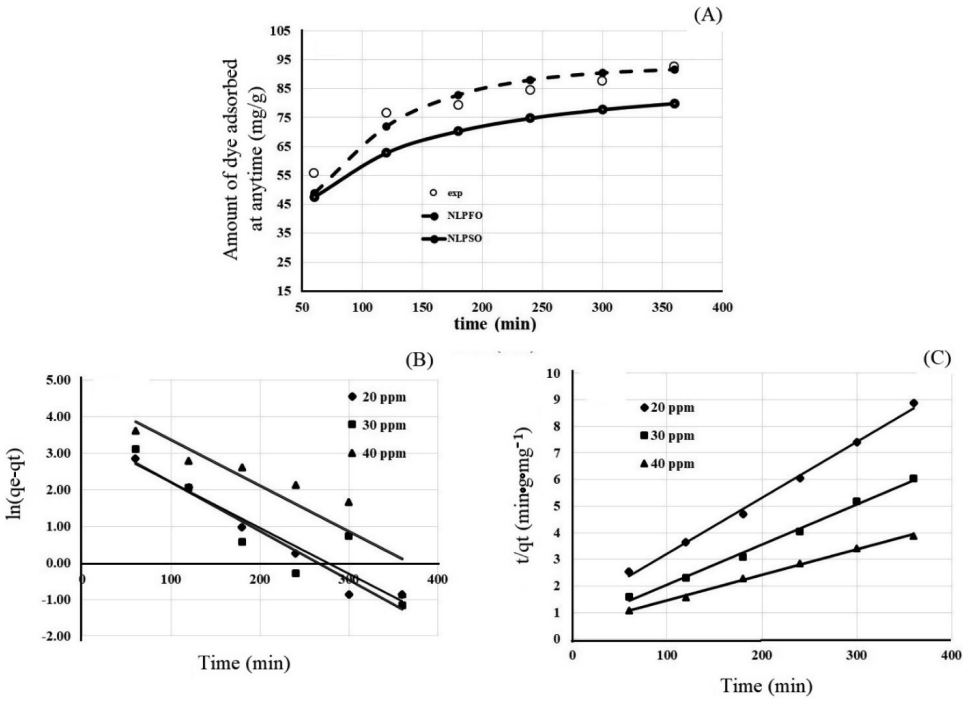

Fig. 9 Pseudo-first-order (PSO) and pseudo-second-order (PSO) plots of alizarin red s (ARS) adsorption onto zeolite L: (A) nonlinear; (B) linear PFO; (C) linear PSO, where C_0 in parts per million (ppm) of ARS and ARY = 40

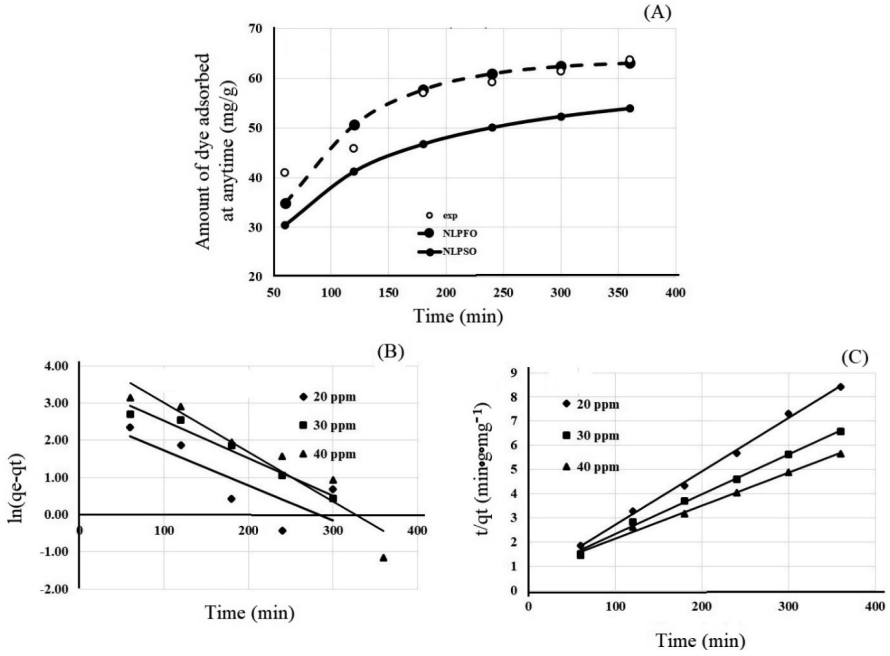

Fig. 10 Pseudo-first-order (PSO) and pseudo-second-order (PSO) plots of alizarin yellow 2G (ARY) adsorption onto zeolite L: (A) nonlinear; (B) linear PFO; (C) linear PSO, where C_0 in parts per million (ppm) of ARS and ARY = 40

suggesting that there was a tendency for the Freundlich model to better fit data at low concentrations and the Langmuir model to better fit higher concentrations. Thus, nonlinear optimization is a mathematically accurate method to determine the adsorption model parameters using the original form of the equation (Ghaffari et al., 2017; López-Luna et al., 2019; Ngakou et al., 2019). In the current work, the NLPFO model seemed to be the most appropriate to describe the adsorption of ARS and ARY onto KLTL. Table 4 demonstrates that the values of Δq were low and the R^2 values were quite high. Furthermore, the value of $q_{t.cal}$ of ARS was derived from the calculation of NLPFO as 91.55 mg/g, which was relatively close to the experimental value of 92.58 mg/g. Conversely, the values of $q_{t.cal}$ of ARY derived from the calculation and experimental values were 63.14 mg/g and 63.69 mg/g, respectively.

Conclusion

Zeolite L (KLTL) was used as an alternative adsorbent for the removal of anionic dye from an aqueous solution. The effects were examined of some parameters (adsorbent dosage, contact time, thermodynamics, and kinetics). Based on the Langmuir adsorption isotherm, the maximum monolayer adsorption capacity levels were 95.24 mg/g and 41.30 mg/g for ARS and ARY, respectively. The thermodynamic study implied that the adsorption of anionic dye onto zeolite L (KLTL) was an endothermic and spontaneous reaction. In addition, the adsorption kinetic results showed that the adsorption process of ARS and ARY onto zeolite L (KLTL) followed a nonlinear pseudo-first-order model. This research indicated that Zeolite L

Table 4 Kinetic parameters of linear and nonlinear models of alizarin red s (ARS) and alizarin yellow 2G (ARY) adsorption onto zeolite L, experimental amount adsorbed ($q_{e(exp)}$) and calculated amount adsorbed ($q_{e(cal)}$)

	Adsorbate	$q_{exp.}$ (mg/g)	Pseudo first order (PFO)				Pseudo Second order (PSO)			
			k_1 (min^{-1})	$q_{t\ cal.}$ (mg/g)	R^2	%Δq	k_2 g/mg/min	$q_{t\ cal.}$ (mg/g)	R^2	%Δq
Linear equation	ARS	92.58	1.25×10^{-2}	12.57	0.8249	0.605	1.90×10^{-4}	104.17	0.9972	9.888
	ARY	63.69	1.32×10^{-2}	11.76	0.9011	0.650	2.40×10^{-4}	73.53	0.9945	12.235
Nonlinear equation	ARS	92.58	7.97×10^{-3}	91.55	0.9571	6.857	1.90×10^{-4}	79.95	0.9881	14.882
	ARY	63.69	8.70×10^{-3}	63.14	0.9493	8.323	2.40×10^{-4}	53.90	0.9909	18.940

R^2 = coefficient of determination; Δq is the standard deviation

(KLTL) could be utilized as an efficient and reasonably priced adsorbent for removing ARS and ARY from an aqueous solution.

Conflict of Interest

The authors declare that there are no conflicts of interest.

Acknowledgments

The Rajamangala University of Technology, Isan Surin Campus provided financial support for this research work.

References

Badran, I., Khalaf, R. 2020. Adsorptive removal of alizarin dye from wastewater using maghemite nanoadsorbents. Sep. Sci. Technol. 55: 2433–2448. doi.org/10.1080/01496395.2019.1634731

Bhomick, P.C., Supong, A., Baruah, M., Pongener, C., Gogoi, C., Sinha, D. 2020. Alizarin red S adsorption onto biomass-based activated carbon: Optimization of adsorption process parameters using Taguchi experimental design. Int. J. Environ. Sci. Technol. 17: 1137–1148. doi.org/10.1007/s13762-019-02389-1

Biglari, H., RodríguezíCouto, S., Khaniabadi, Y.O., Nourmoradi, H., Khoshgoftar, M., Amrane, A., Rashidi, R. 2018. Cationic surfactant-modified clay as an adsorbent for the removal of synthetic dyes from aqueous solutions. Int. J. Chem. React. Eng. 16: 20170064. doi.org/10.1515/ijcre-2017-0064

Fu, F., Gao, Z., Gao, L., Li, D. 2011. Effective adsorption of anionic dye, alizarin red S, from aqueous solutions on activated clay modified by iron oxide. Ind. Eng. Chem. Res. 50: 9712–9717. doi.org/10.1021/ie200524b

Ghaedi, M., Hassanzadeh, A., Kokhdan, S.N. 2011. Multiwalled carbon nanotubes as adsorbents for the kinetic and equilibrium study of the removal of alizarin red S and morin. J. Chem. Eng. Data 56: 2511–2520. doi.org/10.1021/je2000414

Ghaffari, H.R., Pasalari, H., Tajvar, A., Dindarloo, K., Goudarzi, B., Alipour, V., Ghanbarneajd, A. 2017. Linear and nonlinear two-parameter adsorption isotherm modeling: A case-study. Int. J. Eng. Sci. 6: 2319–1805. doi: 10.9790/1813-0609010111

Gholivand, M.B., Yamini, Y., Dayeni, M., Seidi, S., Tahmasebi, E. 2015. Adsorptive removal of alizarin red-S and alizarin yellow GG from aqueous solutions using polypyrrole-coated magnetic nanoparticles. J. Environ. Chem. Eng. 3: 529–540. doi.org/10.1016/j.jece.2015.01.011

Ho, Y.S., McKay, G. 1998. Sorption of dye from aqueous solution by peat. Chem. Eng. J. 70: 115–124. doi.org/10.1016/S0923-0467(98)00076-1

Insuwan, W. 2013. Photophysical properties of cationic and neutral dyes confined in zeolite ltl: Experimental and theoretical studies. Ph.D. thesis. School of Chemistry Institute of Science, Suranaree University of Technology. Nakhon Ratchasima, Thailand.

Insuwan, W., Moonchaisook, K., Junkrin, B. 2020. Removal of textile dye by using activated carbon in aqueous solution. Naresuan University Journal: Science and Technology 28: 10–19. doi: 10.14456/nujst.2020.22

Insuwan, W., Rangsriwatananon, K. 2012. Morphology-controlled synthesis of zeolite and physicochemical properties. Eng. J. 16: 1–12.

Insuwan, W., Rangsriwatananon, K. 2014. Evaluation of adsorption of cationic dyes on H-LTL and K-LTL zeolite. J. Porous Mater. 21: 345–354. doi.org/10.1007/s10934-014-9780-0

Insuwan, W., Saosai, N. 2019. An investigation of phenol adsorption from aqueous solution using solid adsorbents. Naresuan University Journal: Science and Technology 27: 10–19. doi: 10.14456/nujst.2020.22

Jun, K.C., Raman, A.A.A., Buthiyappan, A. 2020. Treatment of oil refinery effluent using bio-adsorbent developed from activated palm kernel shell and zeolite. RSC Adv. 10: 24079–24094. doi.org/10.1039/D0RA03307C

Khayyun, T.S., Mseer, A.H. 2019. Comparison of the experimental results with the Langmuir and Freundlich models for copper removal on limestone adsorbent. Appl. Water Sci. 9: 170. doi.org/10.1007/s13201-019-1061-2

Li, D., Liu, Q., Ma, S., Chang, Z., Zhang, L. 2011. Adsorption of alizarin red S onto nano-sized silica modified with γ-aminopropyltriethoxysilane. Adsorp. Sci. Technol. 29: 289–300.

López-Luna, J., Ramírez-Montes, L.E., Martinez-Vargas, S., et al. 2019. Linear and nonlinear kinetic and isotherm adsorption models for arsenic removal by manganese ferrite nanoparticles. SN Appl. Sci. 1: 950.

Moussout, H., Ahlafi, H., Aazza, M., Maghat, H. 2018. Critical [*sic*] of linear and nonlinear equations of pseudo-first order and pseudo-second order kinetic models. Karbala Int. J. Mod. Sci. 4: 244–254. doi.org/10.1016/j.kijoms.2018.04.001

Ngakou, C.S., Anagho, G.S., Ngomo, H.M. 2019. Non-linear regression analysis for the adsorption kinetics and equilibrium isotherm of phenacetin onto activated carbons. Curr. J. Appl. Sci. Technol. 36: 1–18.

Paul, H., Reginato, A.J., Schumacher, H.R. 1983. Alizarin red S staining as a screening test to detect calcium compounds in synovial fluid. Arthritis Rheum. 26: 191–200. doi.org/10.1002/art.1780260211

Salman, M., Athar, M., Shafique, U., Din, M.I., Rehman, R., Akram, A., Ali, S.Z. 2011. Adsorption modeling of alizarin yellow on untreated and treated charcoal. Turkish J. Eng. Env. Sci. 35: 209–16. doi: 10.3906/muh-1009-32

Slimani, R., Ouahabi, I.E., Benkaddour, S., et al. 2021. Removal efficiency of textile dyes from aqueous solutions using calcined waste of eggshells as eco-friendly adsorbent: Kinetic and thermodynamic studies. Chem. Biochem. Eng. Q. 35: 43–56.

Tsuboy, M.S., Angeli, J.P.F., Mantovani, M.S., Knasmüller, S., Umbuzeiro, G.A., Ribeiro, L. R. 2007. Genotoxic, mutagenic and cytotoxic effects of the commercial dye CI Disperse Blue 291 in the human hepatic cell line HepG2. Toxicol. In Vitro 21: 1650– 1655. doi.org/10.1016/j.tiv.2007.06.020

Venkatesh, S., Arutchelvan, V. 2019. Biosorption of alizarin red dye onto immobilized biomass of *Canna indica*: isotherm, kinetics, and thermodynamic studies. The 1st International Conference on Recent Trends in Clean Technologies for Sustainable Environment. Chennai, India, pp. 409–421.

Yoshida, Y., Shimada, T., Ishida, T., Takagi, S. 2020. Thermodynamic study of the adsorption of acridinium derivatives on the clay surface. RSC Adv. 10: 21360–21368. doi: 10.1039/D0RA03158E

Zhang, Z., Chen, H., Wu, W., Pang, W., Yan, G. 2019. Efficient removal of Alizarin red S from aqueous solution by polyethyleneimine functionalized magnetic carbon nanotubes. Bioresour. Technol. 293: 122100. doi.org/10.1016/j.biortech.2019.122100